

به نام خدا



مرکز دانلود رایگان  
مهندسی متالورژی و مواد

[www.Iran-mavad.com](http://www.Iran-mavad.com)



# 14.1 Ceramics for Biomedical Applications

TADASHI KOKUBO<sup>1</sup>, HYUN-MIN KIM<sup>2</sup> and  
MASAKAZU KAWASHITA<sup>1</sup>

<sup>1</sup>Department of Material Chemistry, Graduate School of Engineering,  
Kyoto University, Yoshida, Sakyo-ku, Kyoto 606-8501, Japan

<sup>2</sup>Department of Ceramic Engineering, School of Advanced Materials Engineering,  
Yonsei University, 134, Shinchon-Dong, Seodaemun-gu, Seoul 120-749, Korea

## 14.1.1 INTRODUCTION

Ceramics are generally defined as being materials based on inorganic substances, and inorganic substances are substances that are not related to living organisms. Nobody, therefore, believed that ceramics could play an important role in repairing living tissues and organs. However, it has been shown over the last three decades, that some ceramics can promote the regeneration of neighbouring tissue, can spontaneously bond to living tissues, and that some ceramics can locally destroy cancer cells so that normal tissue regeneration can occur after treatment. In this chapter, some ceramics which can play an important role in repairing living tissue and organs will be described.

## 14.1.2 CERAMICS FOR ARTIFICIAL JOINTS

Our body is supported by bones from the top of our head to the bottom of our feet. Important organs such as the brain, heart, and lungs are protected from external forces by these bones. We can walk, bend, and grasp objects because our skeletons are comprised of 206 bones, connected through joints.

To achieve these functions, our bones are composed of 99 vol% of an extracellular matrix, and by only 1 vol% of living cells. The extracellular matrix is composed of 50 vol% (or 70 wt%) of inorganic apatite in the form of small, nanometer-sized crystallites, and 50 vol% (or 30 wt%) of organic collagen fibres that are fabricated into a three-dimensional structure, as shown in Figure 14.1.1 [1]. At the joints, bones are covered with a soft cartilage so that they can move smoothly.

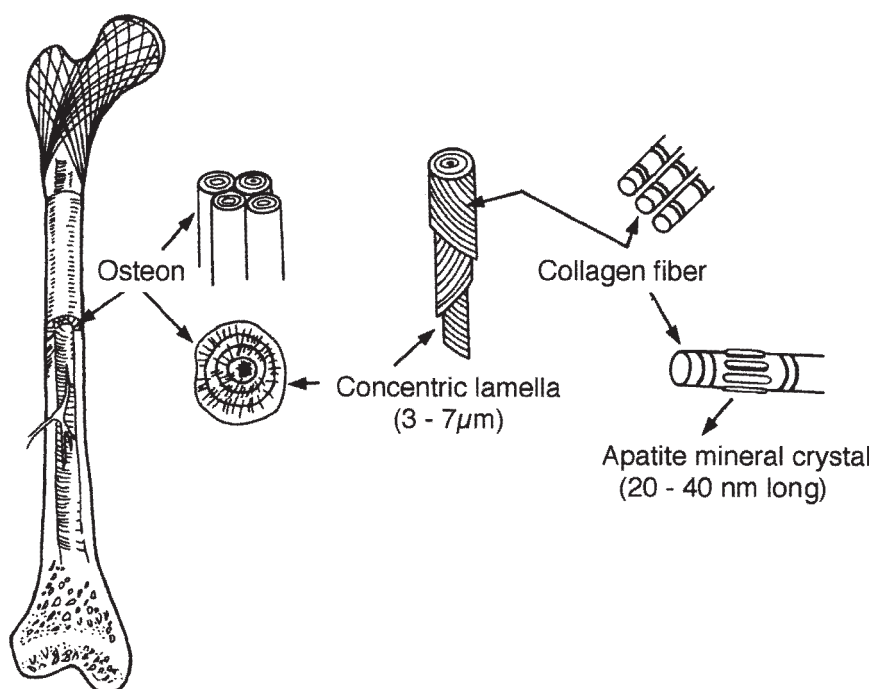


FIGURE 14.1.1 Structure of typical human bone [1].

Bones, and their joints, are sometimes damaged by accidents, disease, aging, etc. When hip and knee joints are damaged, patients sometimes feel severe pain, and have much difficulty in walking, since these joints must slide smoothly at least a few thousand times every day under a load over several times body weight. In such cases, the joints must be replaced with artificial ones. The present number of hip and knee joints replaced with artificial ones total about 100 000 in Japan, and 600 000 in the United States.

The first successful hip joint was developed by Charnley, a British orthopedic surgeon, in 1960. It consisted of a head and stem made of 316 stainless steel, and a cup socket made of ultrahigh molecular weight polyethylene. These were fixed to the surrounding bones by filling the gap between each component and the surrounding bone with a bone cement consisting of polymethylmethacrylate powder and its monomer liquid, and solidifying it *in situ*, as shown in Figure 14.1.2. This was expected to work well for over 20 years. In practice, a loosening of the joint fixation to the surrounding bone was observed within 5–10 years in some cases, and the components had to be retrieved. The reason for this loosening was attributed to wear of the cup and head, and an unstable fixation of the joint components with the bone cement.

Our body fluid contains the same types of ions as those found in seawater [2], although their concentrations are almost a quarter of those of seawater, and our body temperature is higher than that of seawater. Stainless

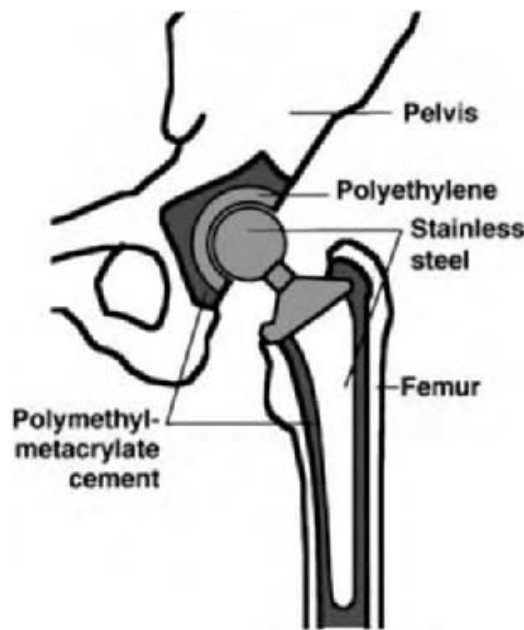


FIGURE 14.1.2 Artificial hip joint system in early 1960s.

steel is liable to corrosion in such circumstances, and so can impart a roughness on the articulating surface of the implant head. As a result, wear debris from the stainless steel head and polyethylene cup were produced, and the coefficient of friction of the articulation increased. The wear debris was phagocytized by macrophages which produced cytokines to induce the resorption of the surrounding bone. In addition, fixation of the joint components to the surrounding bone by the bone cement was not intrinsically stable. The bone cement was encapsulated by a thick membrane of collagen fibres, and had to be isolated from the surrounding bone, because it generated a large amount of heat on solidification from the polymerization of its monomers. The unreacted monomers that were released had an adverse effect on the cardiovascular system. The increased friction gave rise to the extraordinarily large stress at the interface between the components and the surrounding bone, and induced the loosening of the fixed joint.

In 1970, Bautin, a French orthopedic surgeon, replaced both the cup and head of the hip joint with high-density, high-purity sintered alumina [3]. As a result, production of the polyethylene and stainless steel debris was eliminated. The sintered alumina was superior in terms of its mechanical strength, hardness, chemical durability, and hydrophilicity. As a result, the smooth surfaces of the head and cup were maintained for a longer period, and hence, the coefficient of the friction of the articulation was also maintained at a low level over a long period, as shown in Figure 14.1.3 [4]. Later, it was found that even when only the head was made of sintered alumina and the cup was made of polyethylene, as shown in Figure 14.1.4, the production of polyethylene debris and the increase

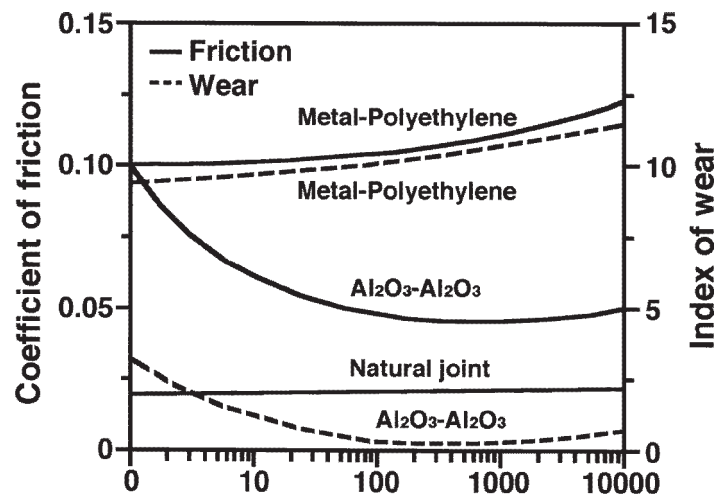


FIGURE 14.1.3 Time dependence of coefficient of friction and wear of alumina-alumina versus metal-polyethylene hip joint in vitro [4].

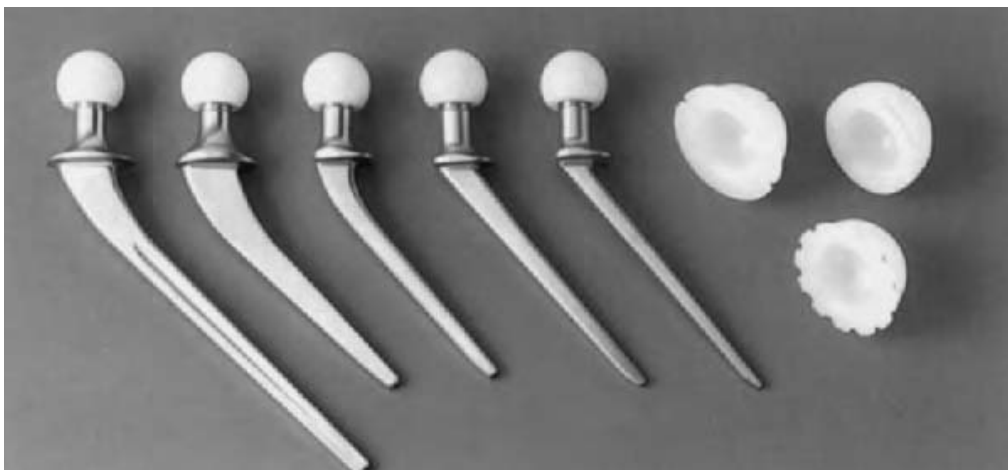


FIGURE 14.1.4 Alumina head (left) and polyethylene cup (right) in hip joint system (photograph courtesy of Kyocera Co., Kyoto, Japan).

in the coefficient of friction of the articulation was remarkably suppressed. Fitting of the head to the cup, both in size and shape, was much easier for this combination than for the ceramic-ceramic combination. Therefore, the alumina-polyethylene combination has been widely used. This combination has also been applied to knee joints.

Recently, however, it has been shown that polyethylene debris produced by this combination can also induce bone resorption over a long period, and these are gradually being replaced with the ceramic-ceramic combination. The mechanical strength of sintered alumina for this use has been improved by suppressing grain growth to achieve a fully dense sintered body, as shown in Table 14.1.1. For this purpose, a small amount of MgO (<0.5%) is added, and

TABLE 14.1.1 Properties of alumina and zirconia ceramics used in surgical implants

Properties	Al <sub>2</sub> O <sub>3</sub> <sup>1</sup>	Y-ZrO <sub>2</sub> <sup>2</sup>	Ce-ZrO <sub>2</sub> /Al <sub>2</sub> O <sub>3</sub> <sup>3</sup>
Density (g/cm <sup>3</sup> )	3.98	6.05	5.57
Average Grain Size (μm)	3.6	0.2–0.4	—
Bending Strength (MPa)	595	1000	1000
Compressive Strength (MPa)	4250	2000	—
Young's Modulus (GPa)	400	150	250
Hardness (HV)	2400	1200	1200
Fracture Toughness (MPa·m <sup>1/2</sup> )	5	7	18

<sup>1</sup>Purity >99.7 wt% [3].

<sup>2</sup>3Y-TZP (3Y<sub>2</sub>O<sub>3</sub>·97ZrO<sub>2</sub> in mol%) [3].

<sup>3</sup>70 vol% of 10Ce-TZP (10CeO<sub>2</sub>·90ZrO<sub>2</sub> in mol%) and 30 vol% of Al<sub>2</sub>O<sub>3</sub> [5].

the total amount of SiO<sub>2</sub> and Na<sub>2</sub>O is suppressed to below 0.1%. The amount of CaO is suppressed to below 0.1% in order to obtain a high resistance to static fatigue.

Other types of ceramics with higher mechanical strength and fracture toughness have also been tested for use for this purpose. Sintered partially stabilized zirconia is one of these materials. It is, however, liable to exhibit a decrease in its mechanical strength due to a transformation of the metastable tetragonal phase to the stable monoclinic phase in an aqueous environment, such as is found in the living body. Sintered zirconia generally shows a lower hardness value than sintered alumina. In addition, radioactive elements such as thorium and uranium emitting α- and γ-rays with a very long half-life, are liable to be contaminants in the zirconium oxide. The phase-transformation problem in zirconia was easily solved by suppressing the grain growth, and the radioactivity of commercially available zirconia ceramics was confirmed to be negligible. Sintered yttrium or magnesium partially stabilized zirconia is already clinically used as the head of hip joints in combination with a polyethylene cup. The use of these zirconia heads in combination with cups made from the same zirconia is controversial with respect to the wear rate of the articulation. A ceria-stabilized zirconia–alumina nanocomposite [5] shows a higher mechanical strength, fracture toughness, hardness, and stability against phase transformation. This ceramic is now being tried for use both as the joint cup and the head. The properties of these zirconia ceramics are listed in Table 14.1.1.

It is believed that the problems of debris and friction in artificial joints could be solved in practical terms in the near future. The remaining problem to be solved is the stable fixation of the components of the artificial joints to the surrounding bone.

### 14.1.3 CERAMICS FOR ARTIFICIAL BONE

Artificial materials implanted into bone defects are generally encapsulated by a tissue of collagen fibres and are isolated from the surrounding bone, as shown in Figure 14.1.5. This is a normal reaction against a foreign presence by the protection mechanism of our bodies. Owing to this encapsulation, artificial material cannot be fixed rigidly to the surrounding bone.

In the early 1970s, Hench showed that some glasses in the  $\text{Na}_2\text{O}-\text{CaO}-\text{SiO}_2-\text{P}_2\text{O}_5$  system spontaneously bonded to living bone without forming any fibrous tissue around them, as shown in Figure 14.1.6 [6, 7]. These glasses were the first man-made materials that had been found to bond to living tissue. They were named Bioglass<sup>®</sup>. Their typical composition (45S5) is  $\text{SiO}_2 = 45$ ,  $\text{Na}_2\text{O} = 24.5$ ,  $\text{CaO} = 24.5$ , and  $\text{P}_2\text{O}_5 = 6$  wt%. Their tensile strength is 42 MPa, whereas that of the human cortical bone is a maximum of 150 MPa, as shown in Table 14.1.2 [8]. Consequently, they are used clinically only in areas under reduced loads, such as periodontal fillers, as shown in Figure 14.1.7 [9].

In 1976, Jarcho *et al.* [10] showed that sintered hydroxyapatite ( $\text{Ca}_{10}(\text{PO}_4)_6(\text{OH})_2$ ) also bonds to living bone. Although it forms a highly dense body that shows a maximum bending strength around 200 MPa, bodies in practical use generally show a bending strength at around 115 MPa, which is lower than that of human cortical bones, as shown in Table 14.1.2 [11]. This ceramic is widely used clinically in the fields of orthopaedics and dentistry, as a bone

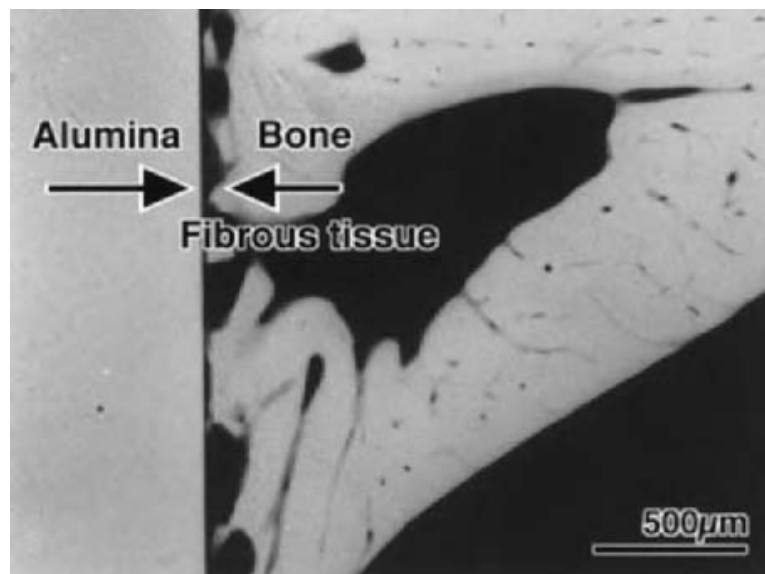


FIGURE 14.1.5 Contact microradiograph of the interface between alumina and rabbit tibial bone (12 weeks after implantation).

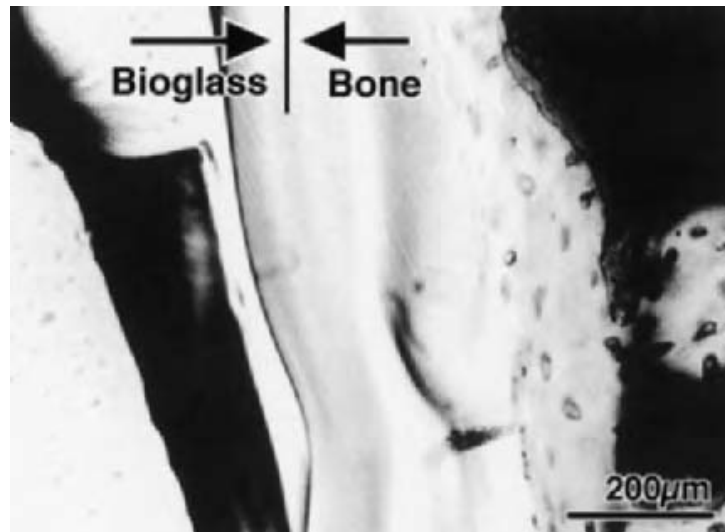


FIGURE 14.1.6 Optical micrograph of the interface between Bioglass 45S5 and rat bone (1 year after implantation) [7].

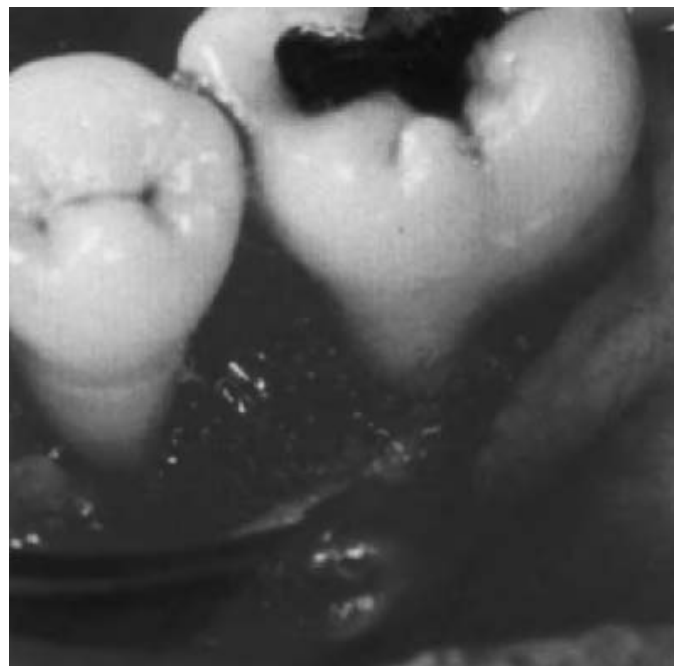


FIGURE 14.1.7 Clinical use of Bioglass as periodontal filler (photograph courtesy of US Biomaterials, Baltimore, MD, USA).

filler in a bulk, or granular form that has a dense, or porous, structure, as shown in Figure 14.1.8 [12].

In 1981, Kokubo *et al.* [13] developed a glass-ceramic containing 38 wt% of crystalline oxyfluoroapatite ( $\text{Ca}_{10}(\text{PO}_4)_6(\text{O}, \text{F}_2)$ ) and 34 wt% of  $\beta$ -wollastonite ( $\text{CaSiO}_3$ ) 50–100 nm in size, in a  $\text{MgO}-\text{CaO}-\text{SiO}_2$  glassy matrix by the sintering and crystallization of a glass powder compact with composition

TABLE 14.1.2 Properties of bioactive ceramics and human bone

Properties	Bioglass 45S5	Sintered hydroxyapatite	Glass-ceramic A-W	Human cortical bone
Composition (wt%)				
Na <sub>2</sub> O	24.5	Ca <sub>10</sub> (PO <sub>4</sub> ) <sub>6</sub> (OH) <sub>2</sub>	0	
MgO	0		4.6	
CaO	24.5		44.7	
SiO <sub>2</sub>	45.0		34.0	
P <sub>2</sub> O <sub>5</sub>	6.0		16.2	
CaF <sub>2</sub>	0		0.5	
Phase				
	Glass	Apatite	Apatite β-Wollastonite Glass	
Density (g/cm <sup>3</sup> )	2.66	3.16	3.07	1.6–2.1
Vicker's hardness (HV)	458	600	680	
Compressive Strength (MPa)		500–1000	1060	100–230
Bending strength (MPa)	42 (Tensile)	115–200	215	50–150
Young's Modulus (GPa)	35	80–110	118	7–30
Fracture Toughness K <sub>IC</sub> (MPa·m <sup>1/2</sup> )		1.0	2.0	2–6
Slow crack growth, <i>n</i>		12–27	33	

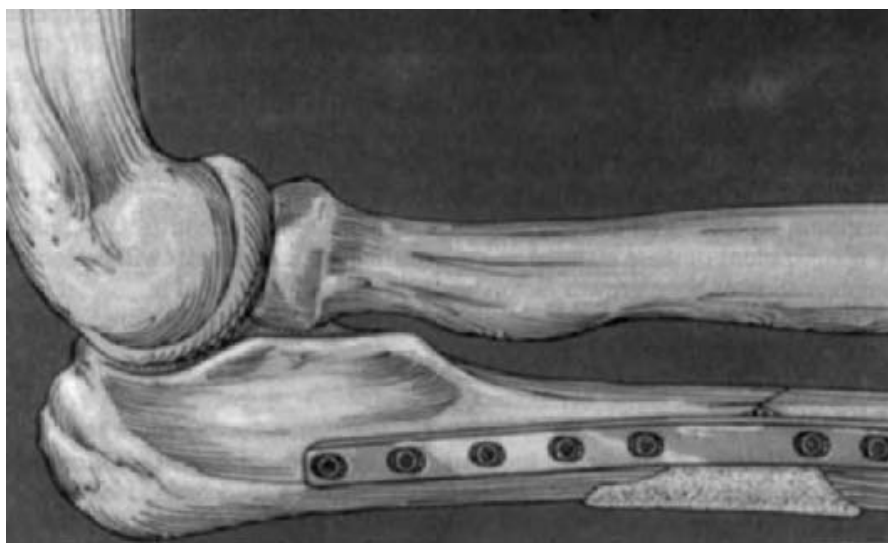


FIGURE 14.1.8 Clinical use of porous sintered hydroxyapatite in forearm fracture treatment [12].

MgO = 4.6, CaO = 44.7, SiO<sub>2</sub> = 34.0, P<sub>2</sub>O<sub>5</sub> = 16.2, and CaF<sub>2</sub> = 0.5 wt%. This glass-ceramic was named A-W, after the names of crystalline phases. It also directly bonds to living bone. The period of time required for the glass-ceramics A-W to bond to living bone was longer than that for Bioglass 45S5, but shorter than that for sintered hydroxyapatite. Its bending strength, 215 MPa, was higher than that of human cortical bones, as shown in Table 14.1.2. It was estimated from the dependence of the bending strength of the glass-ceramic upon stressing rate in a simulated body fluid, that it could withstand usage over 10 years under continuous loading of bending stresses of 65 MPa, where the sintered hydroxyapatite may be broken within 1 min [14]. Glass-ceramic A-W has been used clinically in Japan as artificial vertebrae, intervertebral disks, and iliac crests, etc. since 1991. More than 60 000 patients have received it as a bone substitute. Figure 14.1.9 shows an X-ray photograph of an artificial vertebra which was substituted for the lumbar vertebra of a sheep, and bonded to the surrounding



FIGURE 14.1.9 X-ray photograph of artificial vertebra of glass-ceramic A-W which substituted for a lumbar vertebra of a sheep and bonded to the surrounding cancellous bone (2 years after implantation: photograph courtesy of Professor T. Yamamuro, Kyoto University, Japan).

cancellous bone [15]. These bone-bonding ceramics such as Bioglass<sup>®</sup>, sintered hydroxyapatite, and glass-ceramic A-W, are now called bioactive ceramics.

However, even glass-ceramic A-W cannot replace highly loaded bones such as the femoral and tibial bones, since its fracture toughness of  $2 \text{ MPa m}^{1/2}$  is not so high as that of the human cortical bones at  $6 \text{ MPa m}^{1/2}$ . For these applications, metallic materials such as Ti-6Al-4V alloy coated with hydroxyapatite using a plasma spray method are mainly utilized. In the above technique, however, hydroxyapatite powders are momentarily heated in a flame above  $10\,000^\circ\text{C}$  to be partially molten and decomposed. As a result, a porous layer of calcium phosphate, different from the hydroxyapatite, is weakly bonded to the metallic substrate. Such a layer is not stable in a living body over a long period [16]. Metallic materials with a high fracture toughness are desired to exhibit bioactivity by themselves, without any coating of a foreign material. How is this possible?

#### 14.1.4 REQUIREMENT FOR ARTIFICIAL MATERIAL TO BOND TO LIVING BONE

Using a transmission electron microscope, it can be observed that all the bioactive ceramics described above spontaneously form an apatite layer on their surfaces in the living body and bond to living bone through this apatite layer, as shown in Figure 14.1.10 [17]. This apatite layer can be reproduced on their surfaces even in an acellular simulated body fluid (SBF) with ion concentrations nearly equal to those of the human blood plasma [2], given in Table 14.1.3 [18] and as shown in Figure 14.1.11 [19]. According to detailed analyses using thin film X-ray diffraction and Fourier transform infrared reflection spectra, this surface layer consists of apatite composed of small crystallites with a composition such that the Ca/P atomic ratio (1.65) is smaller than that of stoichiometric apatite (1.67); small concentrations of  $\text{Na}^+$ ,  $\text{Mg}^{2+}$ ,  $\text{Cl}^-$ , and  $\text{CO}_3^{2-}$  ions are also included. These structural and compositional characteristics are very similar to those of bone mineral. Therefore, bone-producing cell, called an osteoblast, can preferentially proliferate and differentiate on its surface to produce apatite and collagen, rather than the fibrous tissue-producing cell called a fibroblast, similar to the surface of fractured bone [20, 21]. Consequently, the surrounding bone comes into direct contact with the surface apatite as shown in Figure 14.1.10. When this occurs, a tight chemical bond is formed between the bone mineral and the surface apatite in order to reduce the interfacial energy between them. It can be concluded from these findings that the essential requirement for an artificial material to bond to bone is the formation of a bone-like apatite layer on its surface in the living body [22, 23]. What kind of materials forms the bonelike apatite layer on their surfaces in the living body?



FIGURE 14.1.10 Transmission electron micrograph of the interface between glass-ceramic A-W and rat tibial bone (8 weeks after implantation).

TABLE 14.1.3 Ion concentrations of human blood plasma and simulated body fluid (SBF)

	Concentration/mM							
	Na <sup>+</sup>	K <sup>+</sup>	Mg <sup>2+</sup>	Ca <sup>2+</sup>	Cl <sup>-</sup>	HCO <sub>3</sub> <sup>-</sup>	HPO <sub>4</sub> <sup>2-</sup>	SO <sub>4</sub> <sup>2-</sup>
Blood plasma	142.0	5.0	1.5	2.5	103.0	27.0	1.0	0.5
SBF*	142.0	5.0	1.5	2.5	148.8	4.2	1.0	0.5

\*Buffered at 7.4 with tris-hydroxymethyl-aminomethane ((CH<sub>2</sub>OH)<sub>3</sub>CNH<sub>3</sub>) and 1M-HCl.

### 14.1.5 REQUIREMENT FOR ARTIFICIAL MATERIAL TO FORM APATITE

Our body fluid is already supersaturated with respect to apatite, even under normal conditions. It can therefore form apatite anywhere in the body. Nevertheless, it is not normally formed except in bone tissue, since the energy barrier for apatite nucleation in the body fluid is generally very high, but is reduced in bone tissue by some cell reactions. Even artificial material, therefore, can form

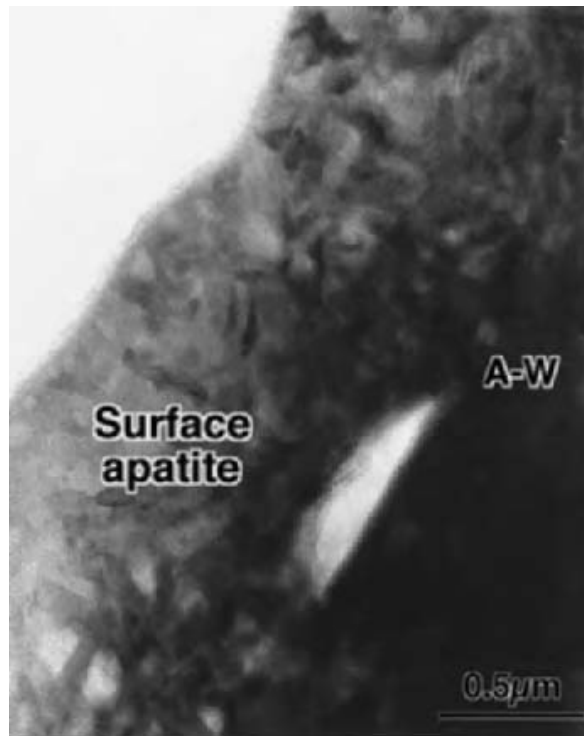


FIGURE 14.1.11 Transmission electron micrograph of the apatite formed on glass-ceramic A-W after soaking in SBF for 3 days.

apatite on its surface, if it has a functional group that can reduce the energy barrier for apatite nucleation, that is, it can induce the heterogeneous nucleation of apatite on its surface.

In the simple ternary system  $\text{CaO-SiO}_2\text{-P}_2\text{O}_5$ , apatite is formed on the surface of  $\text{CaO, SiO}_2$ -based glasses in an SBF, whereas  $\text{CaO, P}_2\text{O}_5$ -based glasses do not form an apatite layer, as shown in Figure 14.1.12 [24]. Apatite formation on the former surface can be interpreted as follows. The  $\text{CaO, SiO}_2$ -based glasses release  $\text{Ca}^{2+}$  ions into the SBF via ion exchange with the  $\text{H}_3\text{O}^+$  ion in the SBF to form  $\text{Si-OH}$  groups, as shown in Figure 14.1.13. The water molecule in the SBF reacts with the  $\text{Si-O-Si}$  bonds in the glass, and breaks the bonds to form  $\text{Si-OH}$  groups. The thus-formed  $\text{Si-OH}$  groups on the surface of the glass then induce apatite nucleation. The released  $\text{Ca}^{2+}$  ions accelerate apatite nucleation by increasing the ionic activity product of the apatite in the SBF, since the  $\text{Ca}^{2+}$  ion is a component of apatite [24]. Once the apatite nuclei are formed, they spontaneously grow by consuming the calcium and phosphate ions from SBF, since the SBF is already supersaturated with respect to apatite. It can be seen from these findings, that an essential requirement for artificial material to form apatite on its surface in the body environment is the presence of functional groups that are effective for apatite nucleation on its surface. Now our problem is, “What kind of functional group is effective for apatite nucleation?”

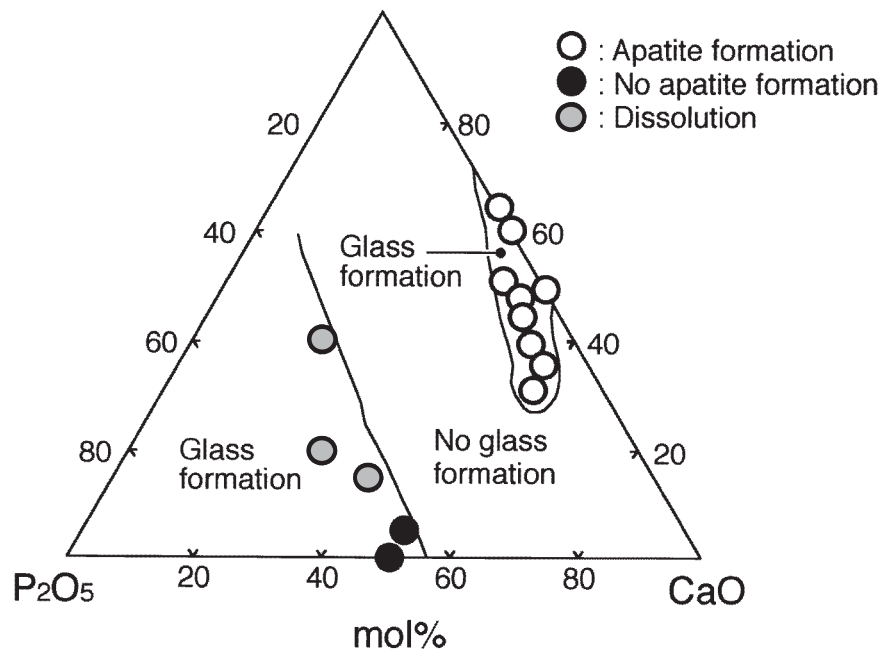


FIGURE 14.1.12 Compositional dependence of apatite formation on CaO–P<sub>2</sub>O<sub>5</sub>–SiO<sub>2</sub> glasses after soaking in SBF for 28 days.

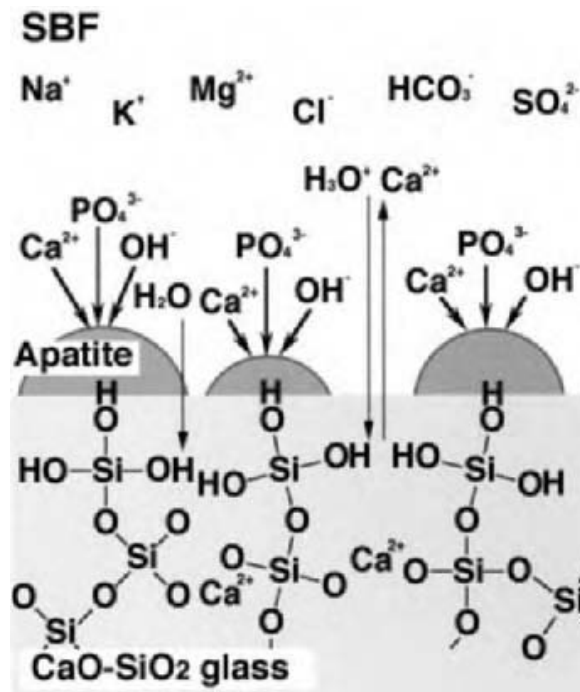


FIGURE 14.1.13 Schematic representation of the mechanism of apatite formation on a CaO–SiO<sub>2</sub> glass in SBF.

### 14.1.6 FUNCTIONAL GROUPS EFFECTIVE FOR APATITE NUCLEATION

Pure metal oxide gels of  $\text{SiO}_2$  [25],  $\text{TiO}_2$  [26],  $\text{ZrO}_2$  [27],  $\text{Nb}_2\text{O}_5$  [28], and  $\text{Ta}_2\text{O}_5$  [29], were all prepared by the sol-gel method, and were found to form a bonelike apatite layer on their surfaces in an SBF, as shown in Figure 14.1.14. However,  $\text{Al}_2\text{O}_3$  gels [26, 30] did not form an apatite layer. This means that functional groups such as  $\text{Si-OH}$ ,  $\text{Ti-OH}$ ,  $\text{Zr-OH}$ ,  $\text{Nb-OH}$ , and  $\text{Ta-OH}$  that are abundant on the surface, are effective for apatite nucleation, but the  $\text{Al-OH}$  group is not. All the former functional groups are negatively charged at values around  $\text{pH} = 7$ , whereas the latter is positively charged.

Not all the gels with the compositions described above, are equally effective for apatite nucleation. For example, an  $\text{SiO}_2$  gel prepared by the hydrolysis and polycondensation of tetraethoxysilane in an aqueous solution containing polyethylene glycol, is more effective than that prepared from pure water, although the structural differences between them cannot be detected using X-ray diffraction and FT-IR [31]. A  $\text{TiO}_2$  gel with the anatase structure, prepared using the sol-gel process and subsequent heat treatment, is much more effective than that with an amorphous or a rutile structure [32]. Tetragonal, or monoclinic,  $\text{ZrO}_2$  gels which were prepared from the sol-gel process and subsequent heat treatments, are much more effective than those with an amorphous or cubic structure [33].

Self-assembled monolayers terminated with  $\text{COOH}$  and  $\text{H}_2\text{PO}_4$  groups, form bone-like apatite on their surfaces in an SBF [34]. This means that  $\text{COOH}$  and  $\text{H}_2\text{PO}_4$  groups are also effective for apatite nucleation. These functional

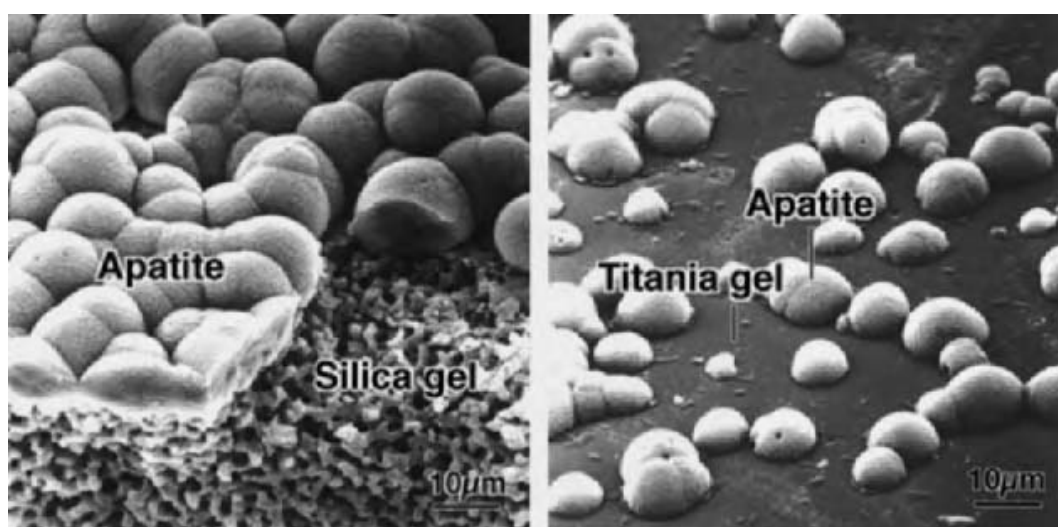


FIGURE 14.1.14 Scanning electron micrographs of the apatite formed on the surfaces of silica gel (left) and titania gel (right) in SBF.

groups also form negatively charged groups in an aqueous solution around  $\text{pH} = 7$ .

On the basis of these findings, we can provide a guide for the apatite-forming ability of various materials, that is, not only ceramics, but also metals and organic polymers that possess the functional groups effective for apatite nucleation on their surfaces, and hence we can obtain bioactive materials with different mechanical properties. In the following sections, some examples of these are described.

### 14.1.7 APATITE-FORMING METALS

Pure titanium metal is generally chemically durable, since it is covered with a passive thin  $\text{TiO}_2$  layer, as shown in Figure 14.1.15a. Even this  $\text{TiO}_2$  layer can react with an NaOH solution to form a sodium titanate hydrogel layer, as shown in Figure 14.1.15b [35, 36]. Although this gel layer is very soft, it can be stabilized as an amorphous sodium titanate layer, as shown in Figure 14.1.15c [35, 36]. It should be noted here, that a graded structure, where the  $\text{Na}_2\text{O}$  content gradually decreases towards the interior, while the Ti content gradually increases towards the interior, is formed within a  $1\ \mu\text{m}$  thick layer at the surface. It is confirmed that the mechanical properties of the titanium metal, including its dynamic fatigue in saline solution, is not adversely affected by the NaOH and heat treatment [37].

It is observed from X-ray photoelectron spectra [38], and from transmission electron microscopy [39], that when the NaOH- and heat-treated titanium metal is soaked in an SBF, it releases  $\text{Na}^+$  ions via ion exchange with the  $\text{H}_3\text{O}^+$  ions in the SBF to form abundant Ti–OH groups on its surface within a short period, as shown in Figure 14.1.16. The thus-formed Ti–OH groups combine immediately with the  $\text{Ca}^{2+}$  ions in the SBF to form an amorphous calcium titanate. Later, these combine with the phosphate ion in the SBF to form an amorphous calcium phosphate with a low Ca/P ratio. The Ca/P ratio increases, to eventually reach a value of 1.65, and transforms into crystalline apatite, as shown in Figure 14.1.16. This apatite formation process is interpreted in terms of the electrostatic reaction of the negatively charged Ti–OH groups on the surface, and the positively charged  $\text{Ca}^{2+}$  ions and the negatively charged phosphate ions in the SBF [40].

The thus-formed apatite nuclei spontaneously grow by consuming the calcium and phosphate ions in the SBF to form a dense, uniform apatite layer, as shown in Figure 14.1.17a. At the interface between the apatite and the titanium metal, a graded structure is formed, where the apatite content gradually decreases, while the Ti content increases toward the interior, as shown

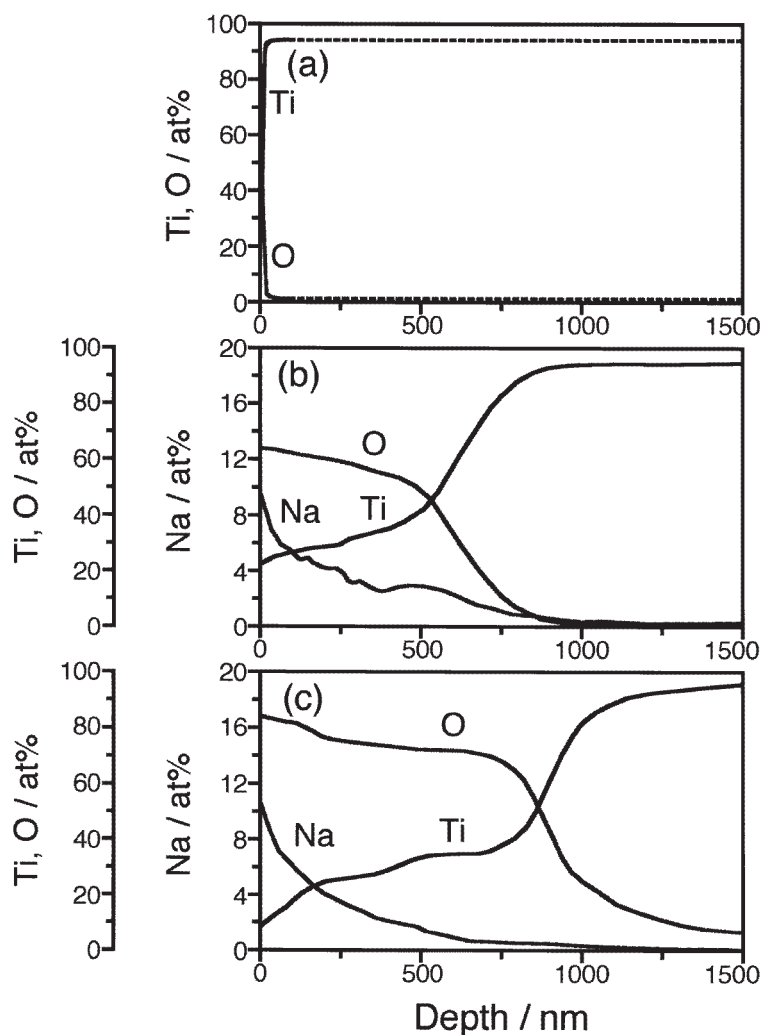


FIGURE 14.1.15 Depth profiles of Auger electron spectroscopy of the surface of titanium metal before (a) and after soaking in 5.0M-NaOH solution for 24 h (b) and subsequent heat treatment at 600°C for 1 h (c).

in Figure 14.1.17b [36]. Consequently, the thus-formed apatite is tightly integrated with the titanium substrate.

The NaOH-and heat-treated titanium metal forms the same apatite layer on its surface even *in vivo*, and tightly bonds to living bone through the apatite layer [41, 42]. For example, when an NaOH-and heat-treated titanium metal rod, 5 mm in diameter and 25 mm in length, was implanted into the intramedullar canal of a rabbit femur, it formed an apatite layer on its surface within 3 weeks, as shown in Figure 14.1.18 [43], and was completely surrounded by living bone within 12 weeks as shown in Figure 14.1.18b [43]. At a period of 12 weeks after implantation, the rod was pulled out from the intramedullar canal, being accompanied by a fragment of the surrounding bone.

It has already been confirmed that similarly treated titanium-based alloys such as, Ti-6Al-4V, Ti-6Al-2Nb-Ta, and Ti-15Mo-5Zr-3Al also form

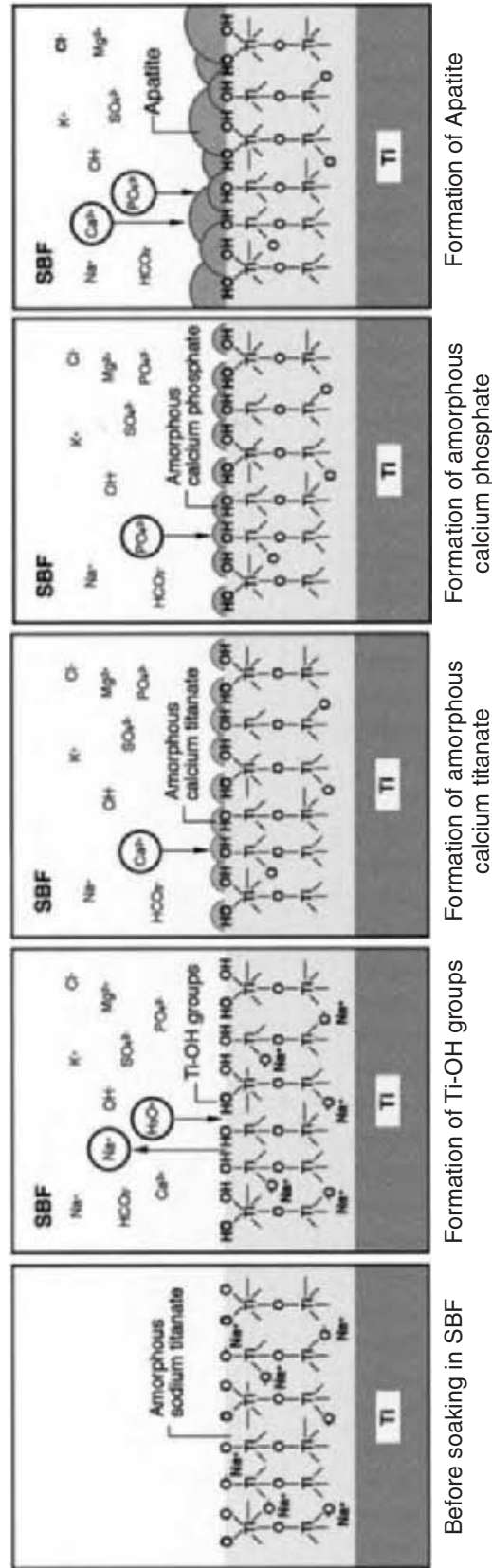


FIGURE 14.1.16 Schematic representation of the mechanism of apatite formation on the NaOH- and heat-treated titanium metal in SBF.

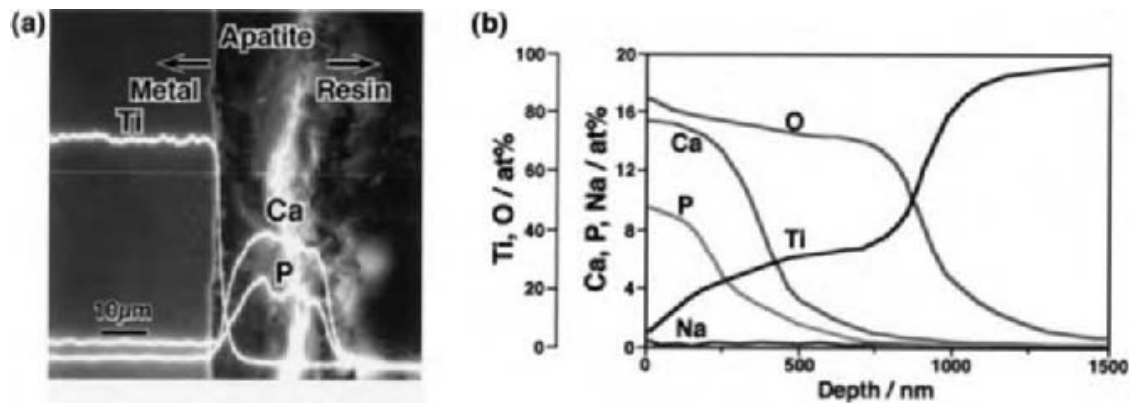


FIGURE 14.1.17 Scanning electron micrograph and energy-dispersive X-ray microanalysis (a) and profile of Auger electron spectroscopy (b) of the cross-section of apatite formed on the NaOH- and heat-treated titanium metal in SBF.

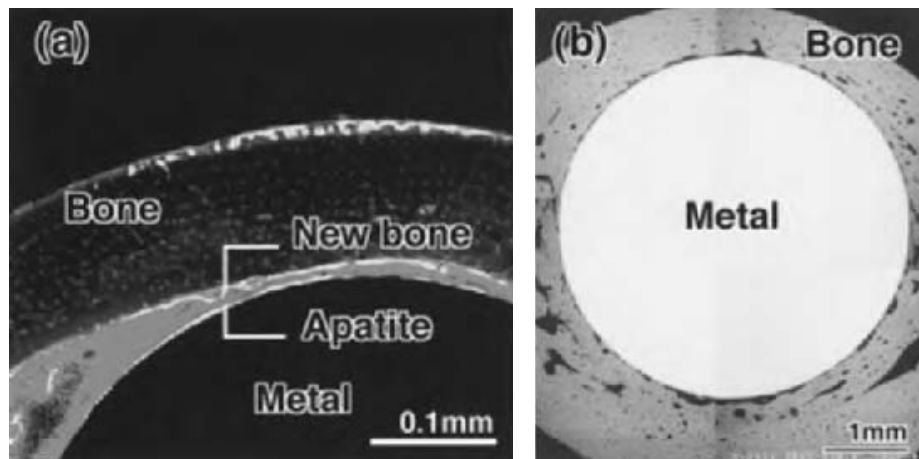


FIGURE 14.1.18 Confocal laser scanning micrograph (a) and scanning electron micrograph (b) of the cross-section of the NaOH- and heat-treated titanium metal rod implanted in intramedullar canal of rabbit femur (3 weeks (a) and 12 weeks (b) after implantation).

bone-like apatite on their surfaces in an SBF, as well as in the living body, and bond to living bone [35, 44].

Tantalum metal also forms an amorphous sodium tantalate layer with a graded structure [45] on treatment with a 0.5 M NaOH solution at 60°C for 24 h [46] and heat treatment at 300°C for 1 h [47]. The thus-treated tantalum metal also forms a bone-like apatite layer on its surface in an SBF as well as in the living body, and bonds to living bone [48].

These bone-bonding metals can be called bioactive metals, since they also form bone-like apatite on their surfaces in the living body, and bond to the living bone, similarly to the bioactive ceramics. These bioactive metals are useful as bone substitutes even under load-bearing conditions, such as hip and knee

joints, vertebrae, and dental implants, since they exhibit bioactivity as well as high fracture toughness. Clinical trials assessing their suitability for application to hip joints are now being conducted. They are expected to be rigidly fixed to the surrounding bone over a long period.

Not only these metals, but also nanocomposites of ceria-stabilized zirconia with alumina show a high mechanical strength as well as high fracture toughness, as shown in Table 14.1.1. The Zr–OH groups here are effective for apatite nucleation, as described in Section 14.1.6. This indicates that ZrO<sub>2</sub>-based composites also can show bioactivity, if a large number of Zr–OH groups are formed on its surface by some suitable chemical treatment. When the zirconia–alumina nanocomposite was treated with a 5 M H<sub>3</sub>PO<sub>4</sub> solution at 95°C for 4 days, many Zr–OH groups were formed on its surface. The thus-treated composite formed a bone-like apatite layer on its surface in an SBF within 7 days [49].

Young's moduli of the metals and zirconia ceramics described above are 100–200 GPa. They are higher than that of human cortical bone. In such cases, the surrounding bone is liable to be resorbed, since the stress is mainly borne by these materials, but not by the surrounding bones. The contemporary desire is to develop bioactive materials with low elastic moduli and ductility.

#### 14.1.8 APATITE–POLYMER COMPOSITE

In order to obtain a bioactive material with a lower elastic modulus and ductility, Bonfield prepared a hydroxyapatite–polyethylene composite [50]. Hydroxyapatite powders can be dispersed in a polyethylene matrix up to 45 vol% without losing any ductility of the polymer. The resultant composite shows a Young's modulus value of about 3 GPa, an ultimate tensile strength of 22–26 MPa, and a fracture toughness,  $K_{IC}$ , of 2.9 MPa m<sup>-1/2</sup> [51]. This composite is already used clinically as an artificial middle ear bone, etc.

#### 14.1.9 APATITE-FORMING INORGANIC–ORGANIC HYBRIDS

CaO–SiO<sub>2</sub> glasses form a bone-like apatite layer on their surfaces in the body, and bond to living bone [52]. It is expected that a ductile bioactive material with a low elastic modulus can be obtained, if some organic molecules can be incorporated into the structure of these glasses. In practice, when an organic molecule such as polydimethylsiloxane (PDMS; HO–[Si(CH<sub>3</sub>)<sub>2</sub>–O]<sub>n</sub>–H) or 3-isocyanatopropyltriethoxysilyl-terminated polytetramethylene oxide (Si-PTMO; (C<sub>2</sub>H<sub>5</sub>O)<sub>3</sub>Si(CH<sub>2</sub>)<sub>3</sub>NHCOO–((CH<sub>2</sub>)<sub>4</sub>O)<sub>n</sub>–CONH(CH<sub>2</sub>)<sub>3</sub>Si(OC<sub>2</sub>H<sub>5</sub>)<sub>3</sub>), is incorporated into the structure of a CaO–SiO<sub>2</sub>–TiO<sub>2</sub> glass by the sol–gel

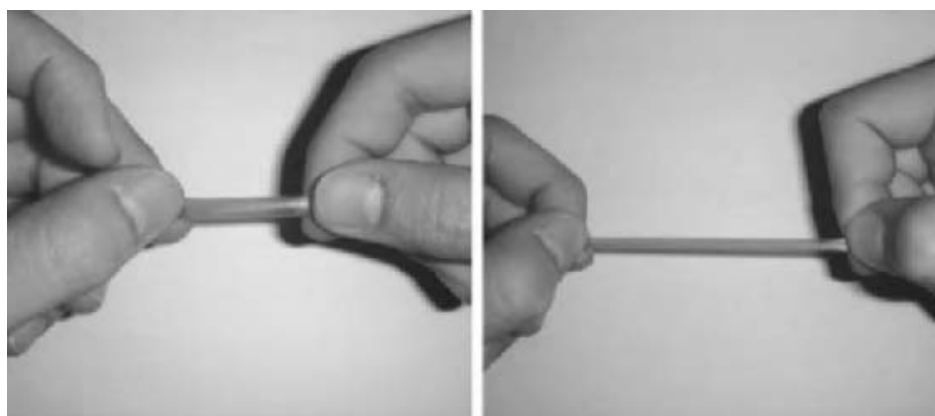


FIGURE 14.1.19 Photographs of PDMS–TiO<sub>2</sub> hybrid with a high deformability (as-prepared (left) and elongated (right)).

process, the resultant hybrids show an apatite-forming ability in an SBF as well as a high ductility [53, 54]. Their mechanical strength is, however, liable to decrease in the body environment.

When a Ca-free PDMS–TiO<sub>2</sub> hybrid was prepared using the sol–gel process, and treated in pure water around 80°C, a hybrid containing anatase-type TiO<sub>2</sub> nanoparticles was obtained. The resultant hybrid showed an apatite-forming ability in an SBF, as well as high deformability, as shown in Figure 14.1.19 [55, 56]. Its mechanical strength was, however, lower than that of human cortical bone.

#### 14.1.10 APATITE–POLYMER FIBER COMPOSITES

In order to obtain a bioactive material with a high mechanical strength, high fracture toughness, low elastic modulus and ductility similar to natural bone, an apatite–polymer fiber composite with a structure analogous to that of the natural bone given in Figure 14.1.1 needs to be fabricated. Such a composite could be obtained, if a synthetic organic polymer fiber was fabricated into a three-dimensional structure analogous to that of the fiber collagen (found in natural bone), and modified with a functional group on its surface known to be effective for apatite nucleation, and then soaked in an SBF, as shown in Figure 14.1.20.

It is already known that a fabric of synthetic organic polymer fiber in a three-dimensional structure can show various mechanical properties by itself [57]. Several attempts have been made to form effective functional groups for apatite nucleation on organic polymers [58, 59]. Most of the resultant polymers, however, form apatite only in solutions that are more highly supersaturated with respect to apatite than SBF, and do not form apatite in

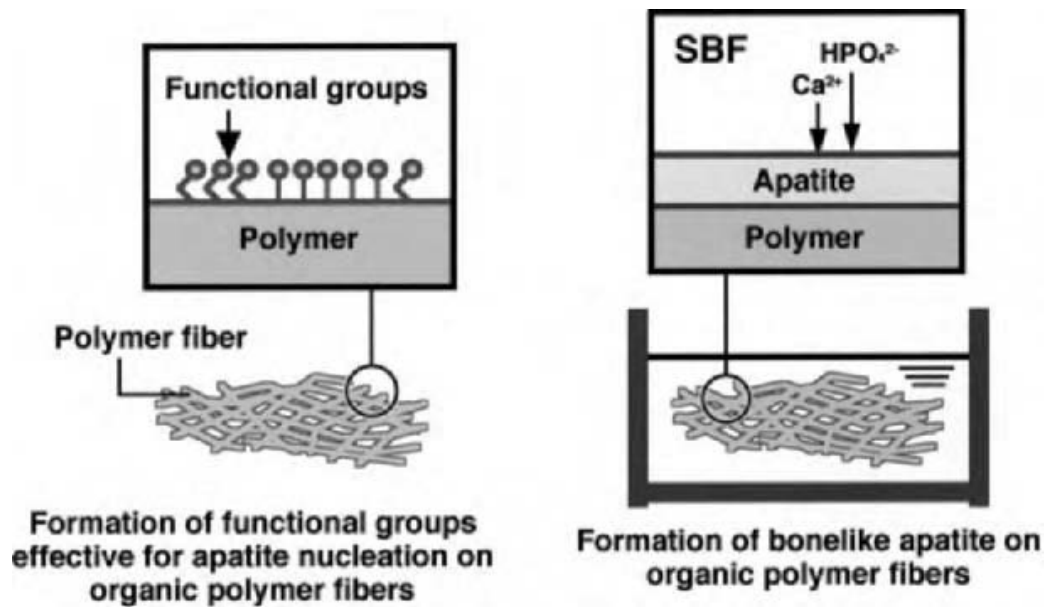


FIGURE 14.1.20 Schematic representation of fabrication process of apatite-polymer composite with analogous three dimensional structure to that of natural bone.

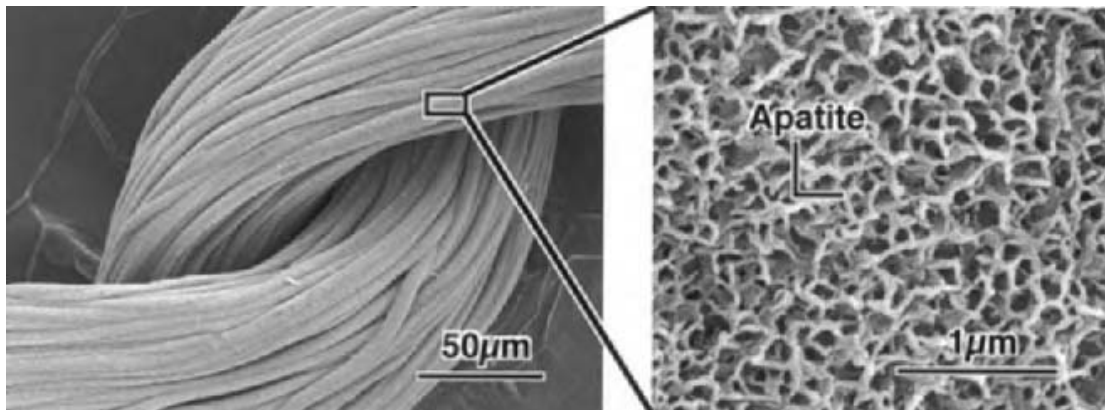


FIGURE 14.1.21 Scanning electron micrograph of EVOH fibers constituting a fabric, which were treated with silane coupling agent and calcium silicate solution, and then soaked in SBF for 2 days.

SBF. Apatite formed in solutions different from an SBF in ion concentrations, is different from bone mineral in its composition and structure [60].

Recently, it was shown that ethylene–vinyl alcohol copolymer (EVOH) fibers constituting a fabric, formed small bone-like apatite crystallites on their surfaces in an SBF, when they were modified with a silane coupling agent and a CaO–SiO<sub>2</sub> gel on their surfaces, as shown in Figure 14.1.21 [61]. The same polymer also formed bonelike apatite on its surface in an SBF, when it was modified by a titania gel on its surface, and treated in hot water around 80°C to precipitate anatase [62].

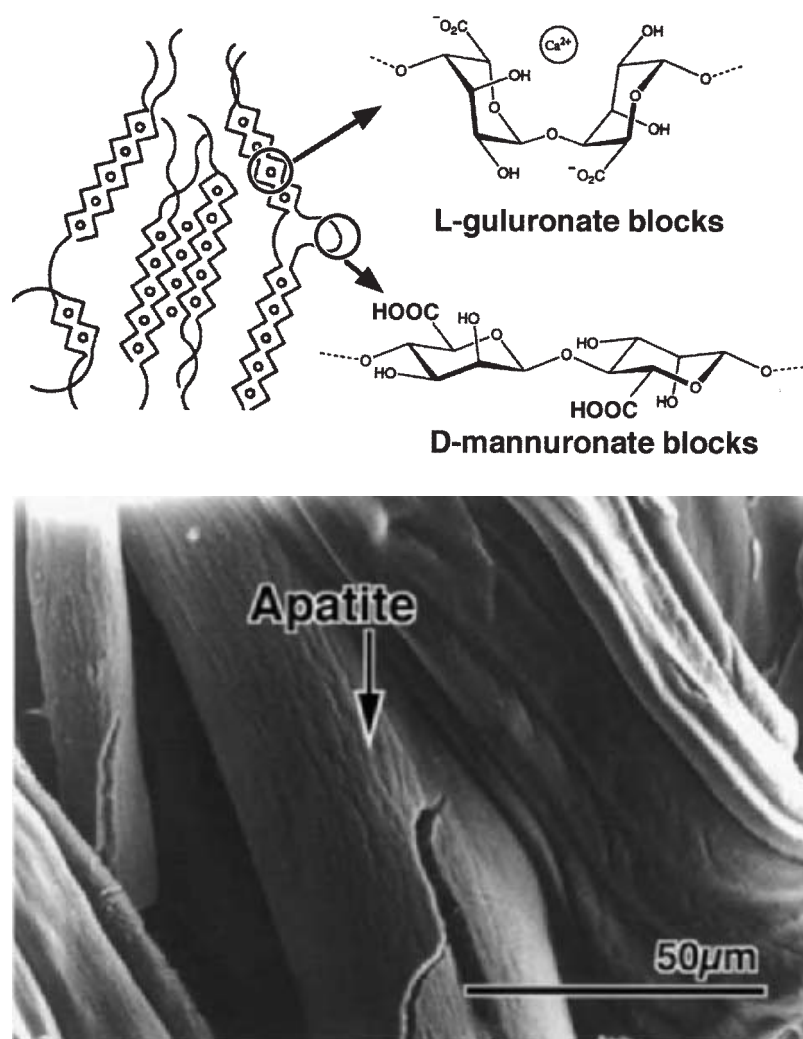


FIGURE 14.1.22 Structure and calcium alginate fiber (top) and scanning electron micrograph of apatite formed on the fiber (left).

The COOH group is also effective for apatite nucleation, as described in Section 14.1.6. Alginic acid possesses the COOH group in its structure, as shown in Figure 14.1.22. Therefore, its fibres form bone-like apatite on its surface in an SBF within 7 days, when they are previously treated in an aqueous saturated  $\text{Ca}(\text{OH})_2$  solution, as shown in Figure 14.1.22 (Kokubo, unpublished). Chitin fibres can be modified to form COOH groups on their surfaces by carboxymethylation. They also form apatite on their surfaces in an SBF within 7 days, when they are previously treated in an aqueous saturated  $\text{Ca}(\text{OH})_2$  solution [63].

Homogeneous deposition of the apatite on the individual fibers constituting a fabric in a three-dimensional structure is being attempted. The resultant composite is expected to exhibit analogous mechanical and biological properties to those of the natural bone.

TABLE 14.1.4 Some bioactive cements

Powder	Liquid	Reference
Tetracalcium phosphate ( $\text{Ca}_4(\text{PO}_4)_2\text{O}$ )	Sodium phosphate	Chow, 1998
Dicalcium phosphate anhydrate ( $\text{CaHPO}_4$ )	aqueous solution	
$\alpha$ -Tricalcium phosphate ( $\alpha\text{-Ca}_3(\text{PO}_4)_2$ )	Sodium phosphate	Chow, 1998
Calcium carbonate ( $\text{CaCO}_3$ )	aqueous solution	
Monocalcium phosphate monohydrate ( $\text{Ca}(\text{H}_2\text{PO}_4)_2 \cdot \text{H}_2\text{O}$ )		
$\alpha$ -Tricalcium phosphate ( $\alpha\text{-Ca}_3(\text{PO}_4)_2$ )	Sodium succinate	Asaoka, 1999
Dicalcium phosphate dihydrate ( $\text{CaHPO}_4 \cdot 2\text{H}_2\text{O}$ )	aqueous solution	
Tetracalcium phosphate ( $\text{Ca}_4(\text{PO}_4)_2\text{O}$ )	Sodium chondroitin sulfate aqueous solution	

### 14.1.11 BIOACTIVE CEMENTS

Bone defects sometimes exhibit complex shapes. Bioactive cements are useful for repairing such defects, and are usually composed of powder and liquid. When the powder and liquid are mixed in an appropriate ratio, they show fluidity, and in a few minutes, they solidify, forming bone-like apatite, and later bond to the surrounding living bone. They can be injected into the bone defects as a viscous liquid, or filled into the bone defects as a paste. Typical examples of these are given in Table 14.1.4 [64, 65]. All these cements set within 5–10 min after being mixed, forming bone-like apatite, and later bond to the living bone. Their compressive strengths after setting are in the range 60–90 MPa. They are already widely used in clinical applications. Various attempts to improve their mechanical strengths are still being carried out.

### 14.1.12 CERAMICS FOR *IN SITU* RADIOTHERAPY OF CANCERS

The most popular cancer treatment is the excision of the diseased part by surgery. Once an organ is excised, however, its full function is hardly recovered. The development of a cancer treatment, in which only the cancer cells are destroyed locally, so that the normal tissue can regenerate after treatment, is desired.

Radiotherapy is one treatment with such potential. Conventionally, however, irradiation has been performed externally. As a result, an inadequate radiation dosage could be given to deep-seated cancers, and the normal tissues near the surface of the body could be damaged.

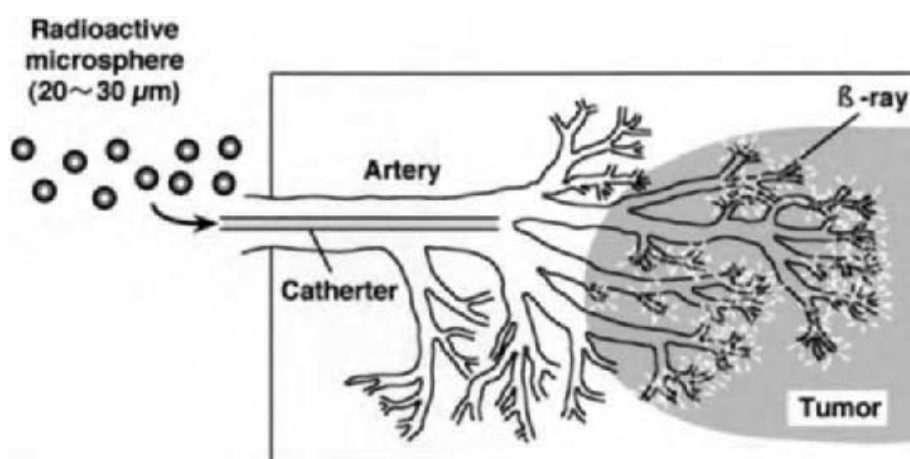


FIGURE 14.1.23 *In situ* cancer treatment using a radioactive microsphere.

In 1987, Erhardt *et al.* [66] showed that  $17\text{Y}_2\text{O}_3-19\text{Al}_2\text{O}_3-64\text{SiO}_2$  (mol%) glass microspheres were useful for *in situ* radiotherapy. These glass microspheres can be prepared using the conventional melting technique, and are not radioactive as prepared. Yttrium-89 ( $^{89}\text{Y}$ ) present in this glass, can be activated by neutron bombardment to form  $^{90}\text{Y}$ , which is a  $\beta$ -emitter with a half-life of 64.1 h. When these glass microspheres, 20–30  $\mu\text{m}$  in size, are dispersed into a saline, and injected into a liver tumour through the hepatic artery by a catheter, as shown in Figure 14.1.23, they are entrapped in a capillary bed in the tumor. As a result, they shut off the blood supply to the tumour and directly, and locally, irradiate the surrounding tumour with the  $\beta$ -rays to destroy the cancer cells. Since  $\beta$ -rays transmit only 5–10 mm in living tissue, it does not have any adverse effect on the normal tissue. This glass has a high chemical durability, and hence releases hardly any of the radioactive  $^{90}\text{Y}$  into the living tissue, and does not damage the normal tissue. The radioactivity of this glass decays to a normal level within 21 days after the neutron bombardment. These microspheres are already used clinically for the treatment of liver cancer in the United States, Canada, and China [67]. The  $\text{Y}_2\text{O}_3$  content in the microsphere is limited to only 17 mol% when the microsphere is prepared by the conventional melting technique for glasses. In addition, the half-life of  $^{90}\text{Y}$  is too short. Consequently, the radioactivity of the microspheres may substantially decay even before the cancer treatment.

Recently, Kawashita *et al.* [68] successfully prepared pure  $\text{Y}_2\text{O}_3$  crystalline microspheres 20–30  $\mu\text{m}$  in size by using a high-frequency induced thermal plasma melting technique, as shown in Figure 14.1.24. Phosphorus-31 ( $^{31}\text{P}$ ) is also not usually radioactive, but can be activated by neutron bombardment to form  $^{32}\text{P}$ , which is a  $\beta$ -emitter with a half-life of a little over 14.3 days. It is expected that microspheres containing  $\text{P}_2\text{O}_5$  will be more effective for *in situ* radiotherapy. The high-frequency induced thermal plasma melting technique has also been used to prepare  $\text{YPO}_4$  crystalline microspheres, 20–30  $\mu\text{m}$  in

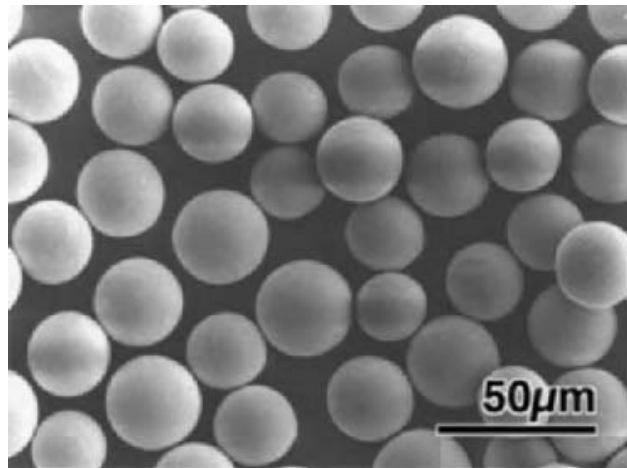


FIGURE 14.1.24 Scanning electron micrograph of  $Y_2O_3$  microspheres.

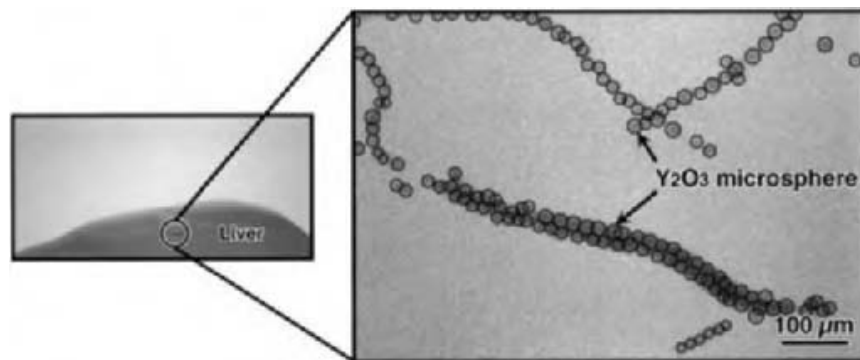


FIGURE 14.1.25 X-ray photograph of  $Y_2O_3$  microspheres which were entrapped in the capillary bed of a rabbit liver.

size [68]. Both of these microspheres have already been confirmed to be highly chemically durable. They are now the subjects of animal experiments for *in situ* radiotherapy of liver cancer. Figure 14.1.25 shows an X-ray photograph of  $Y_2O_3$  microspheres that were entrapped in the capillary bed of the liver of a rabbit.

Liver cancer is the third main cause of death by cancer in Japan. More than 30 000 patients die from liver cancer each year. The development of effective treatments for liver cancer without any side effects is most desirable.

### 14.1.13 CERAMICS FOR *IN SITU* HYPERTHERMIA THERAPY OF CANCER

Cancer cells are destroyed when they are heated up to about  $43^\circ\text{C}$ , and that is only  $6^\circ\text{C}$  above the normal body temperature, whereas normal cells are not damaged up to  $48^\circ\text{C}$ . In addition, a tumour is preferentially heated, as nerve and blood systems are not fully developed in a tumour. Therefore, hyperthermia

therapy can also be an effective non-invasive treatment for cancer. Conventionally, however, heat treatment has been performed externally by using hot water, infrared rays, ultrasonic waves, and electromagnetic microwave radiation, etc. It is difficult to heat deep-seated cancers both effectively and locally. The normal tissue near to the surface of the body can be damaged.

Magnetic fields can penetrate into living tissue without being absorbed by it. Ferro- or ferrimagnetic materials generate heat under an alternating magnetic field in an amount proportional to the area of magnetic hysteresis loop and frequency of the magnetic field. Therefore, when ferro- or ferrimagnetic materials with high chemical durabilities are implanted around tumors and placed under an alternating magnetic field, the tumors can be locally heated up to 43°C and be destroyed by the magnetic hysteresis loss.

Ebisawa *et al.* [69] developed a glass-ceramic containing 36 wt% of magnetite ( $\text{Fe}_3\text{O}_4$ ) crystal particles 200 nm in size, in a  $\text{CaO-SiO}_2$ -based matrix by crystallization of a  $19.50\text{Fe}_2\text{O}_3-40.25\text{CaO}-40.25\text{SiO}_2-3.35\text{B}_2\text{O}_3-1.65\text{P}_2\text{O}_5$  (molar ratio) glass. This showed ferrimagnetism with saturation magnetization of 32 emu/g, and a coercive force of 120 Oe. Heat generation of this glass-ceramic under an alternating magnetic field of 300 Oe at a frequency of 100 kHz, was estimated to be 10 W/g [70]. A pin, 5 cm in length and 3 mm in diameter, was inserted into the medullary canal of a rabbit tibia transplanted with bone tumour, and subjected to an alternating magnetic field of 300 Oe at 100 kHz for 50 min. It was confirmed 3 weeks later that the cancer cells in the medullary canal were completely killed, and that the shape and function of the bone were recovered, as shown in Figure 14.1.26 [71].

Such treatment, however, cannot be applied to humans, since cancers metastasize by this kind of treatment. For humans, ferro- or ferrimagnetic materials must be implanted around the tumors through the vascular system in a type of microsphere, similar to that seen for the radioactive materials. In these cases, the efficiency of the heat generation of the magnetic material must be further increased. Pure magnetite microspheres, 20–30  $\mu\text{m}$  in size, can also be prepared by the high-frequency induced thermal plasma melting technique described above. These show a saturation magnetization as high as 92 emu/g, but show a small coercive force of only 50 Oe, since they consist of magnetite particles as large as 1  $\mu\text{m}$ . Consequently, their heat generation capacity under the same alternating magnetic field as described above, is 10 W/g. When goethite ( $\text{FeOOH}$ ) was deposited on silica microspheres 12  $\mu\text{m}$  in size, in an aqueous solution, and then heat-treated at 600°C in an atmosphere of  $70\text{CO}_2 \cdot 30\text{H}_2$ , microspheres 20–30  $\mu\text{m}$  in size deposited with magnetite were obtained [72]. They show a little smaller saturation magnetization of 53 emu/g, but a large coercive force of 156 Oe, since they consist of magnetite particles as small as 50 nm. Consequently, these show heat generation as large as 41 W/g. Their hysteresis curves under a magnetic field of 300 Oe are shown in Figure 14.1.27



FIGURE 14.1.26 X-ray photograph of rabbit tibial bone transplanted with bone tumor, 5 weeks after the transplantation, (a) No treatment, (b) A ferrimagnetic glass-ceramic pin was inserted into the medullary canal and placed under an alternating magnetic field for 50 min, 2 weeks after the transplantation.

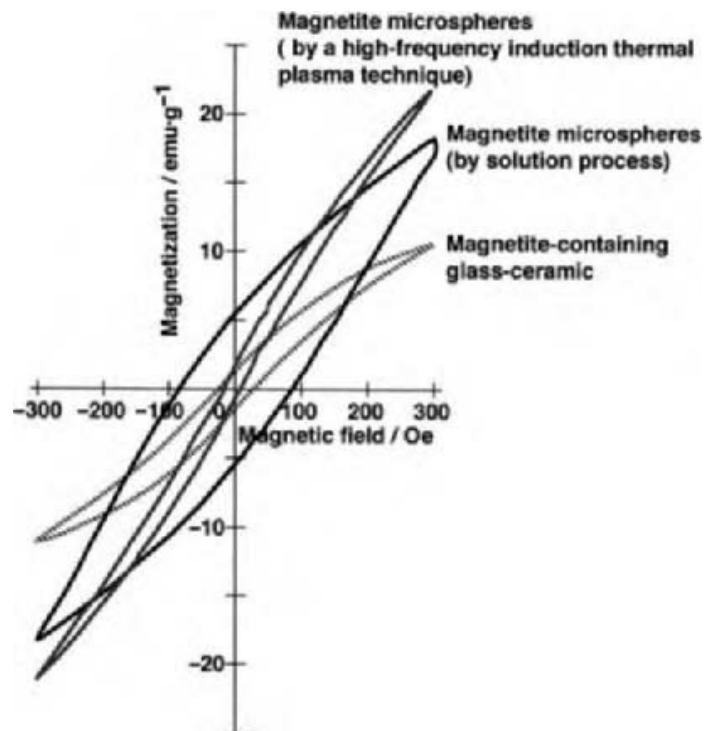


FIGURE 14.1.27 Hysteresis loops of magnetite-containing glass-ceramic, and magnetite microspheres prepared using a high-frequency induction thermal plasma technique and a solution process.

for comparison. The preparation of microspheres consisting of pure magnetite around 50 nm in size is being attempted, to obtain thermoseeds effective for *in situ* hyperthermia therapy.

#### 14.1.14 SUMMARY

Various types of novel materials based on inorganic substances have been developed for biomedical applications over the last three decades. Some of them already play an important, and indispensable role in repairing bone defects, and in cancer treatments. New, advanced ceramic-based materials are expected to be developed for minimally invasive medical treatments in the future.

#### REFERENCES

1. Park, J. B., and Lakes, R. S. (1992). *Biomaterials: An Introduction*, 2nd edn, New York: Plenum.
2. Gamble, J. (1967). *Chemical Anatomy, Physiology and Pathology of Extracellular Fluid*, 6th edn, Harvard University Press.
3. Hulbert, S. F. (1993). The use of alumina and zirconia in surgical implants, *An Introduction to Bioceramics*, pp. 25–40, Hench, L. L., and Wilson, J., eds., Singapore: World Scientific.
4. Hench, L. L. (1991). Bioceramics from concept to clinic. *J. Am. Ceram. Soc.* 74: 1487–1510.
5. Nawa, M., Nakamoto, S., Sekino, T., and Niihara, K. (1998). Tough and strong Ce-TZP/ alumina nanocomposites doped with titania. *Ceram. Int.* 24: 497–506.
6. Hench, L. L., Splinter, R. J., Allen, W. C., and Greenlee, T. K. (1972). Bonding mechanisms at the interface of ceramic prosthetic materials. *J. Biomed. Mater. Res. Symp.* 2: 117–141.
7. Hench, L. L., and Clark, A. E. (1982). Adhesion to bone, *Biocompatibility of Orthopaedic Implants*, Vol. II, pp. 129–170, Boca Raton, FL: CRC Press.
8. Hench, L. L., and Andersson, Ö. (1993). Bioactive glass, *An Introduction to Bioceramics*, pp. 41–62, Hench, L. L., and Wilson, J., eds., Singapore: World Scientific.
9. Wilson, J., Yli-Urpo, A., and Happonen, R.-P. (1993). Bioactive glasses: clinical applications, *An Introduction to Bioceramics*, pp. 63–73, Hench, L. L., and Wilson, J., eds., Singapore: World Scientific.
10. Jarcho, M., Kay, J. F., Drobeck, H. P., and Doremus, R. H. (1976). Tissue, cellular and subcellular events at bone-ceramic hydroxyapatite interface. *J. Bioeng.* 1: 79–92.
11. LeGeros, R. Z., and LeGeros, J. P. (1993). Dense hydroxyapatite, *An Introduction to Bioceramics*, pp. 139–180, Hench, L. L., and Wilson, J., eds., Singapore: World Scientific.
12. Shors, E. C., and Holmes, R. E. (1993). Porous hydroxyapatite, *An Introduction to Bioceramics*, pp. 181–198, Hench, L. L., and Wilson, J., eds., Singapore: World Scientific.
13. Kokubo, T., Shigematsu, M., Nagashima, Y., Tashiro, M., and Higashi, S. (1982). Apatite-and wollastonite-containing glass-ceramic for prosthetic application. *Bull. Inst. Chem. Res. Kyoto Univ.* 60: 260–268.
14. Kokubo, T. (1993). A/W glass-ceramic: processing and properties, *An Introduction to Bioceramics*, pp. 75–88, Hench, L. L., and Wilson, J., eds., Singapore: World Scientific.
15. Yamamuro, T. (1993). A/W glass-ceramic: clinical applications, *An Introduction to Bioceramics*, pp. 89–104, Hench, L. L., and Wilson, J., eds., Singapore: World Scientific.